Paper No. 91. (quote when citing this article)
Eleventh World Conference on Earthquake Engineering
ISBN: 0 08 042822 3

OPTIMAL DECISION STRATEGIES CONTROL OF NONLINEAR STRUCTURAL RESPONSE

CHRISTOPHER V. WHITE[1] and JOHN F. ABEL[1]
JAMES S. THORP[2]

[1]School of Civil and Environmental Engineering, Cornell University
[2]School of Electrical Engineering, Cornell University
Ithaca, NY 14853-3501 USA

ABSTRACT

Many active control algorithms are based on the assumption of linear structural response. This paper presents a control algorithm - Optimal Decision Strategies (ODS) - suitable for use with either linear or nonlinear systems. ODS is a model-reference, pointwise optimal control law requiring the on-line solution of a constrained minimization problem for each update of control forces. Among the advantages of ODS are that an accurate model of the structure is not required, full state measurements are not needed, and control objectives are specified naturally through the reference model. Numerical simulations demonstrate the feasibility of the new control method

KEYWORDS

dynamics, active control, vibration damping, nonlinear, saturation, reference model, semi-rigid connection

INTRODUCTION

The majority of structural control algorithms published in the literature assume linear structural response, regardless of the fact that all structures exhibit inherently nonlinear behavior, especially when subjected to strong ground motion. The critical need for new algorithms for nonlinear structures has been highlighted in proceedings of several international conferences and workshops on structural control (for example WCSC, 1994). One potential candidate for controlling nonlinear structures, known as Optimal Decision Strategies Control (ODS), is presented in this paper.

Previous applications of ODS have been in the field of electric power systems (Thomas et al., 1976), and robotics (Spong et al., 1986, Spong et al., 1987) where conditions of low state dimensionally and full sensing and actuation are typical. Numerical simulations and physical experiments with three-link rigid-arm robots have demonstrated the feasibility of ODS in this context.

The purpose of this paper is to extend the ODS concept to a new class of problems; namely civil engineering structures. In contrast to the robot, civil structures have high state dimensionality, numerical rather than closed-form state equations, and a limited number of sensors and actuators. This paper presents the analytical formulation which allows ODS to be applied when a sensor and controller are not available at every degree of freedom. More extensive information on ODS can be found in the first author's Ph.D. dissertation (White, 1995).

System Equations

Consider a multi-degree-of-freedom structure with the following system of discretized 1st-order nonlinear equations of motion:

$$\dot{\mathbf{x}}(t) = \mathbf{f}(\mathbf{x},t) + \mathbf{G}\mathbf{u}(t) \tag{1}$$

$$\mathbf{x} = \begin{bmatrix} \mathbf{q}(t) \\ \dot{\mathbf{q}}(t) \end{bmatrix}; \quad \mathbf{f} = \begin{bmatrix} \dot{\mathbf{q}}(t) \\ \mathbf{f}_2(\mathbf{x},t) \end{bmatrix}; \quad \mathbf{G} = \begin{bmatrix} \mathbf{0} \\ \mathbf{M}^{-1}\mathbf{g} \end{bmatrix} \tag{2}$$

where $\mathbf{x} = [\, q_1(t), \ \ldots, \ q_n(t), \dot{q}_1(t), \ \ldots, \ \dot{q}_n(t) \,]^T$ is the state vector, $\mathbf{f}_2 = [\, \mathbf{M}^{-1}(-\mathbf{f}_D - \mathbf{f}_R + \mathbf{f}_E) \,]^T$ is the *n-by-1* vector of mass-normalized damping, restoring, and externally applied forces, $\mathbf{M} > 0$ is the symmetric *n-by-n* mass matrix, $\mathbf{u}(t)$ is the *m-by-1* control vector, and $\mathbf{g}$ is the *n-by-m* control influence vector. In general, $\mathbf{f}_2(\mathbf{x},t)$ is a nonlinear function of the state vector having multiple equilibrium points.

It is assumed that the m control inputs are bounded so that $|u_i| \le u_{i_{max}}$, and that there are m state measurements. Let the m measured state variables comprise the output vector, $\mathbf{y}$. The state vector and the equations of motion are partitioned into measured and unmeasured states so that $\mathbf{x} = [\mathbf{x}_m \ \mathbf{x}_u]^T = [\mathbf{q}_m \ \mathbf{q}_u \ \dot{\mathbf{q}}_m \ \dot{\mathbf{q}}_u]^T$, and the terms $\mathbf{f}_2(\mathbf{x},t)$ and $\mathbf{M}^{-1}\mathbf{g}$ appearing in Eq. 2 are written in partitioned form as

$$\mathbf{f}_2 = \begin{bmatrix} \mathbf{f}_m(\mathbf{x}_m, \mathbf{x}_u, t \\ \mathbf{f}_u(\mathbf{x}_m, \mathbf{x}_u, t) \end{bmatrix} \tag{3}$$

$$\mathbf{M}^{-1}\mathbf{g} = \begin{bmatrix} \mathbf{M}_m^{-1}\mathbf{g}_m \\ \mathbf{0} \end{bmatrix} = \begin{bmatrix} \mathbf{G}_m \\ \mathbf{0} \end{bmatrix} \tag{4}$$

It is assumed that the control inputs are independent so that the *m-by-m* matrix $\mathbf{G}_m^T\mathbf{G}_m > 0$ and that $\mathbf{G}_m(\mathbf{G}_m^T\mathbf{G}_m)^{-1}\mathbf{G}_m^T$ is the identity matrix.

ODS Objective Function

As the response of the structure evolves in time, the derivative of the output vector $\dot{\mathbf{y}}$ traces out a trajectory. Imagine that at a series of discrete time points, a more desirable "reference" trajectory is defined, by whatever means, by the vector $\mathbf{v}$ (to be discussed in the next section). Consider the situation at some time instant t = T, and define as $\alpha(T)$ the set of all output derivatives instantaneously achievable under the translation by $\mathbf{u}(T)$ according to Eq. 1, given the constraints on $\mathbf{u}(T)$. The *Optimal Decision Strategy* is to choose that $\mathbf{u}(T)$ from among the admissible set of $\mathbf{u}(T)$, that makes $\dot{\mathbf{y}}$ track $\mathbf{v}$ as closely as possible. This is formulated in terms of the L_2 norm as

$$\min_{\mathbf{u}} \| \alpha(T) - \mathbf{v}(T) \| \tag{5}$$

For notational simplicity, the time index T is henceforth suppressed, and the optimization is understood to occur at discrete time points. Control force $\mathbf{u}$ is held constant between optimization points.

The objective function is written as an explicit function of $\mathbf{u}$ by substituting the state equations, Eq. 1. However, the entire top partition of Eq. 1 is an identity, and is not subjected to control explicitly, so that certain terms in the expansion of Eq. 5 drop out. The explicit form of the objective function becomes

$$\min_{\mathbf{u}}\left\{\frac{1}{2}\mathbf{u}^T\mathbf{P}\mathbf{u}+\left[\mathbf{B}\left(\begin{bmatrix}\dot{\mathbf{q}}_m\\ \mathbf{f}_m(\mathbf{x}_m,\mathbf{x}_u)\end{bmatrix}-\begin{bmatrix}\mathbf{v}_1\\ \mathbf{v}_2\end{bmatrix}\right)\right]^T\mathbf{u}\right\} \tag{6}$$

$$|u_1| \le u_{i_{max}}$$

in which

$$\mathbf{P}=\mathbf{G}_m^T\mathbf{G}_m \quad \text{and} \quad \mathbf{B}=\left[\mathbf{G}_m^T\ \mathbf{G}_m^T\right]$$

Equation 6 is a quadratic programming problem with linear inequality constraints. The dimension of the solution vector **u** is equal to the number of control actuators operating on the structure. Thus, although the dimension of the structure is large, the size of the optimization problem is small.

Reference Trajectory

The control law generated by solution of Eq. 6 at discrete time points is largely determined by the choice of reference trajectory, **v**. Various choices of **v**, including $\mathbf{v} = \mathbf{0}$, have been investigated. Experience has shown that an effective control results when **v** is chosen so as to lead the output derivative $\dot{\mathbf{y}}$ along a trajectory which is in some sense natural for the structure. This can be accomplished through use of a reference model which is compatible with the structure, but exhibits improved dynamic characteristics such as linear behavior with increased viscous damping. Such a reference trajectory is computed on-line at each discrete time point from the following expression:

$$\mathbf{v}=\dot{\mathbf{x}}^r+\mathbf{A}^r(\mathbf{y}-\mathbf{x}^r) \tag{7}$$

in which **y** is the measured output vector and $\mathbf{x}^r$ is the state of a reference model, which satisfies the following equation of motion:

$$\dot{\mathbf{x}}^r=\mathbf{A}^r\mathbf{x}^r \tag{8}$$

If Eq. 8 is substituted into Eq. 7 the simpler form of

$$\mathbf{v}=\mathbf{A}^r\mathbf{y} \tag{9}$$

results. It can be seen that the reference trajectory is solely a function of the reference model and the measured structural response, and is independent of any externally applied load. Therefore, it is neither necessary to preplan **v** off-line using an assumed excitation, nor to simulate the evolution of the reference model on-line, in order to compute the reference trajectory.

Clearly, the reference model must have dimension consistent with **y** in order for Eq. 9 to be meaningful. Of interest is the case when $m << n$, that is, only a small number of state variables are measured. One way to create a reference compatible with the structure is to apply a model order reduction technique to a linearized finite element model of the structure. Modal truncation is a popular way of forming a reduced-order model, but is inappropriate in the present context because with modal truncation, reduction takes place on generalized *modal* coordinates, rather than on physical coordinates (in which the measured responses are available). The appropriate class of reduction techniques for creating an effective reference model is exemplified by Guyan/Irons reduction, sometimes known as *static condensation*. One method that improves on Guyan/Irons reduction is the IRS method (O'Callahan 1989), and this method is selected for use in the present work.

In summary, the reference trajectory is given by Eq. 9, in which $\mathbf{A}^r$ is a reference model possessing dynamic properties which would be desirable for the actual structure to possess. The suitable form for this reference model is given as

$$\mathbf{A}^r=\begin{bmatrix}\mathbf{0} & \mathbf{I}\\ -(\mathbf{M}^r)^{-1}\mathbf{K}^r & -(\mathbf{M}^r)^{-1}\mathbf{C}^r\end{bmatrix} \tag{10}$$

in which $\mathbf{M}^r$, $\mathbf{K}^r$, and $\mathbf{C}^r$ are *m-by-m* mass, stiffness, and damping matrices.

If $\mathbf{v}$ is generated as proposed here from Eqs. 9 and 10, the top partition $\mathbf{v}_1$ is equal to the velocity of the measured state variables, $\dot{\mathbf{q}}_m$, so that the objective function of Eq. 6 reduces even further to the simpler form

$$\min_{\mathbf{u}}\left\{\frac{1}{2}\mathbf{u}^T\mathbf{P}\mathbf{u}+\left[\mathbf{G}_m^T(\mathbf{f}_m(\mathbf{x}_m,\mathbf{x}_u)-\mathbf{v}_2)\right]^T\mathbf{u}\right\} \tag{11}$$

$$|u_i| \le u_{i_{max}}$$

ON-LINE OPTIMIZATION

A modified version of Hildreth's primal/dual method (Hildreth, 1957) is used to solve Eq. 11 iteratively for the optimal control vector $\mathbf{u}$ at each optimization point. Hildreth's method optimizes one coordinate of the solution vector at a time through the same iterative process used by the Gauss/Seidel method of solving systems of linear algebraic equations. Inequality constraints are explicitly satisfied at each iteration. To increase computational efficiency, Hildreth's original algorithm has been modified to solve for the primary variables directly, rather than solving for their duals first.

To illustrate the method, let $J(\mathbf{u})=\frac{1}{2}\mathbf{u}^T\mathbf{P}\mathbf{u}+\mathbf{b}^T\mathbf{u}, \mathbf{P}>\mathbf{0}$, be the objective function and let $\mathbf{u}$ be the state vector in R^m. Take an arbitrary $\mathbf{u}^0$. Obtain a $\mathbf{u}^1$ by minimizing J($\mathbf{u}$) with respect to each component of $\mathbf{u}$ in turn while holding other components fixed at their last obtained values. $\mathbf{u}^2$ is similarly obtained from $\mathbf{u}^1$, etc. In general, $\mathbf{u}^{p+1}$ is found from $\mathbf{u}^p$ by

$$u_i^{p+1}=\begin{cases} w_i^{p+1} & \text{if } \left|w_i^{p+1}\right| \le u_{i\,max} \\ \text{sgn}(w_i^{p+1})u_{i\,max} & \text{if } \left|w_i^{p+1}\right| > u_{i\,max} \end{cases} \tag{12}$$

in which

$$w_i^{p+1}=-\frac{1}{P_{ii}}\left(\sum_{j=1}^{i-1}P_{ij}u_j^{p+1}+\sum_{j=i+1}^{m}P_{ij}u_j^p+\frac{b_i}{2}\right) \tag{13}$$

and $i=1,2,...m;\ p = 0,1,2,....$ Iteration is terminated after a maximum number of iterations or when a suitably accurate solution has been found. The positive definite nature of $\mathbf{P}$ guarantees a unique solution. The motivation for choosing Hildreth's method lies in its simplicity and its rapid speed of solution for small problems.

EXAMPLE

A five story structure shown in Fig. 1 will be used to illustrate the effectiveness of the control scheme. The structure is a strong column-weak beam steel frame modelled with 31 nodes and 38 beam-column elements, having a total of 84 unrestrained degrees of freedom (DOF). The structure supports dead and live loads, and including the applied loads and the self-weight of the steel frame, has a total weight of 1890 kN (450 kips).

Each beam-column connection is modelled with inelastic, semi-rigid Top-Seat-Angle-Web (TSAW) connections to provide the frame with a strong nonlinear response. The connections are modelled as discrete rotational springs with an inelastic moment-rotation curve modelled by the force-space bounding-surface plasticity model. Each connection is assumed to have a nominal strength equal to 80% of the beam it connects. Other connection parameters such as initial and ultimate stiffness are computed from a set of normalized moment-rotation design curves constructed by Deierlein et al. (1991) from the computerized database of Kishi et al. (1986).
Control forces are applied through active hydraulic bracing with horizontally mounted actuators, placed

along the center column line of the two-bay frame, one between each of the five stories. Semi-active bracings of a similar configuration have already been used on actual buildings, and are a viable means of applying control forces. Horizontal displacement and velocity of the five nodes along the center column line comprise the output vector.

The reference model (Eq. 10) is constructed from the full 84-DOF model by first linearizing about the origin then reducing to the same five DOF of the output vector using the IRS reduction technique. The frequencies of the actual (linearized) model are compared to the reference model frequencies in Table 1. The excellent accuracy of the IRS reduction technique is evident.

Table 1. Natural frequencies (Hz)

Mode	Actual	Ref. Model
1	1.08	1.08
2	3.24	3.24
3	6.14	6.14
4	9.89	9.86
5	13.6	13.6

An advantage of the proposed ODS control law is that the design objective is specified in clearly meaningful terms through the reference model. For this example, the reference model is assigned 50% critical viscous damping in the first three modes, and 2% damping in modes 4 and 5. The 50% is chosen to provide a substantial, but not unrealistic, control effect. The *design objective* is to control the actual nonlinear structure to respond exactly as a simplified linear structure with 50% viscous damping in the first three modes of vibration.

The structure is subjected to the first 20 seconds of the 1952 Taft earthquake, scaled to a PGA = 0.76g, PGV of 75 cm/sec. Transient analysis is performed using the Newmark-β method with a time step of 0.005 seconds. The control forces are updated every 0.01 seconds.

Analysis Results

The effect of the control on the displacement of the roof is illustrated in Fig. 2, and shows a 65% reduction in peak displacement. Note the permanent drift that is present in the uncontrolled response is not present in the controlled response.

Hysteresis loops of three exterior TSAW connections are compared in Fig. 3. While the demands on the connection are greatly reduced, the inherent nonlinear response of the building is not eliminated, confirming that the controller is not simply keeping the nonlinear system within linear range, but is operating on a fully nonlinear, hysteretic system.

Figure 4 illustrates the excellent ability of the control to achieve its design objective. The heavy curve is the roof displacement actually achieved, the thin curve is the displacement of an 84 DOF model, linearized about the origin, having 50% damping in three modes. The two curves of this figure very nearly coincide; the slight discrepancies are attributed to approximations inherent in specifying the design objective through the simplified 5 DOF reference model. It is emphasized that in the uncontrolled design objective (thin curve) the structure is linear, whereas in the controlled case, even though the response matches that of the linear structure, the structure is nonlinear.

Peak story drifts (interstory displacement divided by story height) are shown graphically in Fig. 5, and tabulated along with peak total acceleration and peak control requests in Table 2. Note that in this case, with dead and live loads applied to the frame, peak control forces for the lowermost actuator are equal to 39% of the frame's total weight of 1890 kN.

Effects of Control Saturation

To demonstrate the effects of a further nonlinearity, control saturation, all five actuators are set to saturate at 500 kN, then at 300 kN. Peak story drifts are listed in Table 3 for the two different levels of constraint, and compared to the performance of the unconstrained controller. The power required for the controller is

calculated by multiplying the control force by the piston velocity for each actuator, then summing up for all five actuators. The unconstrained controller requires a peak power of 900 kW.

Table 2. Peak uncontrolled and controlled response values

Floor	StoryDrift (%)		Total Acc. (g)		U_{max} (kN)
	U = 0	U≠ 0	U = 0	U ≠ 0	U ≠0
4-5	1.56	0.45	1.51	0.83	165
3-4	1.54	0.54	0.93	0.79	364
2-3	1.58	0.67	1.01	0.74	505
1-2	1.33	0.68	0.93	0.74	600
G-1	0.66	0.41	0.83	0.76	653

When the constraint level is set to 500 kN, which represents a decrease of 23% from the optimal (unconstrained) maximum control force, the story drifts increase 3.3% over the unconstrained case, with a drop in the peak power consumption of 7.1% to 840 kW. A 300 kN saturation limit corresponds to a 54% decrease in peak control force, a story drift increase of 25%, and a peak power decrease of 29% to 640 kW.

Rather than using the same size actuators for all floors in the building, economy can be achieved by sizing the actuators according to the force demand. Therefore, the actuators between floors 4-5 and 3-4 are are set to saturate at 250 kN, while the three remaining actuators between floors 2-3, 1-2, and G-1 are assigned a 450 kN saturation limit. These saturation limits represent a decrease of 31% from the peak unconstrained control forces of 364 kN and 653 kN, occurring at floors 3-4 and G-1, respectively. As seen from the columns labeled "Mix" in Table 3, the increase in story drift averaged over the five floors is only 10%. The power required with this arrangement of actuator sizes 770 kW, a reduction of 15% from the unconstrained value of 900 kW. These data are summarized in Table 4.

While firm conclusions cannot be drawn from such a limited analysis, it appears as though the maximum control force can be limited by as much as 25% without a severe degradation in performance. At the very least, these results illustrate that peak control force requirements alone are not a sufficient metric for comparison of different control strategies.

Table 3. Peak story drift and control forces for various saturation levels

Floor	Story Drift (%)				Max. Control Request			
	∞	500 kN	300 kN	Mix	∞	500 kN	300 kN	(Mix)kN
4-5	0.45	0.47	0.58	0.52	165	164	165	151
3-4	0.54	0.56	0.69	0.61	364	357	279	250
2-3	0.67	0.69	0.84	0.73	505	469	300	394
1-2	0.68	0.70	0.85	0.72	599	500	300	450
G-1	0.41	0.42	0.50	0.43	653	500	300	450

Table 4. Change in performance due to control saturation

Sat. Level	U_{max}	Story Drift	Power
500 kN	-23 %	+3.3 %	-7.1 %
300 kN	-54 %	25 %	-29 %
Mix	-31 %	+10 %	-15 %

CONCLUSION

It has been shown in this paper that ODS can be reformulated and applied to problems for which there are a small number of sensors and actuators, yet no analytical state equations are available. Among the advantages of ODS control are that: (1) an accurate model of the nonlinear structure is not necessary, (2) control objectives are specified in a natural way through a reference model, (3) full state measurements are not needed, and (4) when one or more control inputs are saturated, an optimal distribution of control is maintained.

The numerical results confirm the effectiveness of the new control law, even when the structure has a strongly nonlinear response. The ability of ODS to handle control input saturation in a rational and optimal manner is confirmed, and it is demonstrated that economy can be achieved by sensibly allowing actuators to saturate.

REFERENCES

Deierlein, G.G., Hsieh, S-H., Shen, Y-J., and Abel, J. F. (1991). Nonlinear analysis of steel frames with semi-rigid connections using the capacity spectrum method. Technical Report NCEER-91-0008, NCEER, State University of New York at Buffalo.

Hildreth, C. (1957). A quadratic programming procedure. Naval Research Quarterly, 4;79-85.

Kishi, N. and Chen, W.F. (1986). Data base on steel beam-to-column connections. Technical Report CE-STR-86-26, School of Civil Engineering, Purdue University.

O'Callahan, J. (1989). A procedure for an improved reduced system (IRS) model. Proceedings of the 7th International Modal Analysis Conference, 17-21.

Spong, M., Thorp, J. S., and Kleinwaks, J. (1986). The control of robot manipulators with bounded input. IEEE Transactions on Automatic Control. AC-31(6):483-489.

Spong, M., Thorp, J. S., and Kleinwaks, J. (1987). Robust microprocessor control of robot manipulators. Automatica, 23(3):373-379.

Thomas, R. J., Thorp, J. S., and Pottle, C. (1976). A model-referenced controller for stabilizing large transient swings in power systems. IEEE Transactions on Automatic Control, AC-21:746-750.

WCSC (1994). Proceedings of the First World Conference on Structural Control, IASC.

White, C. V. (1995). Optimal decision strategies for active control of nonlinear structural response. Ph.D. dissertation, Cornell University, Ithaca, NY.

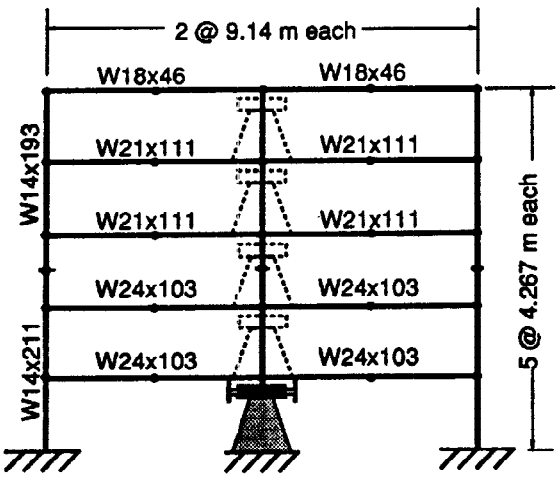

Fig. 1 Example structure with nonlinear TSAW beam-column connections and active bracing between each floor.

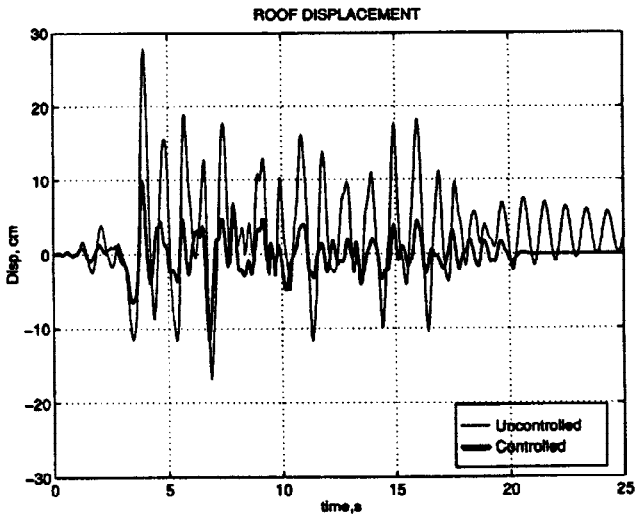

Fig. 2. Lateral roof displacement, center column line.

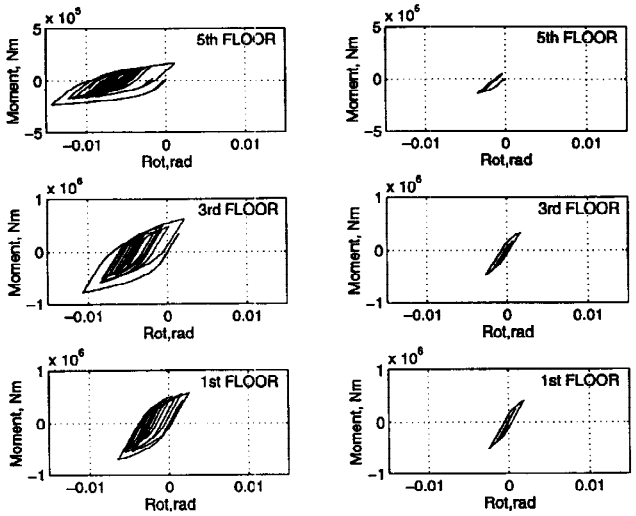

Fig. 3. Hysteresis loops of exterior connections. Left side uncontrolled, right side controled.

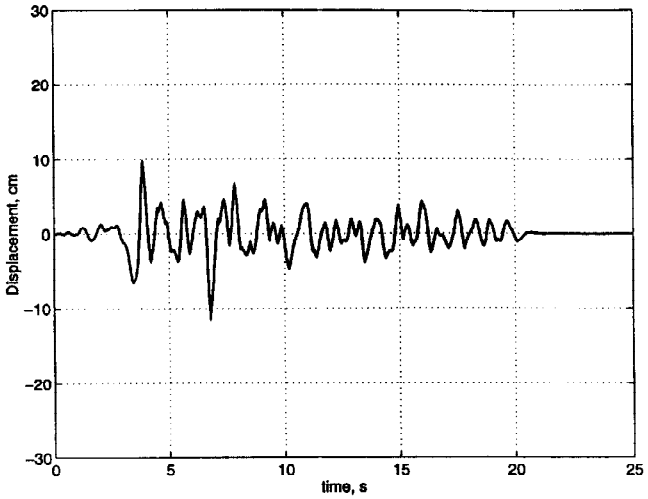

Fig. 4. Design objective compared to achieved response, lateral roof displacement. The curves nearly coincide.

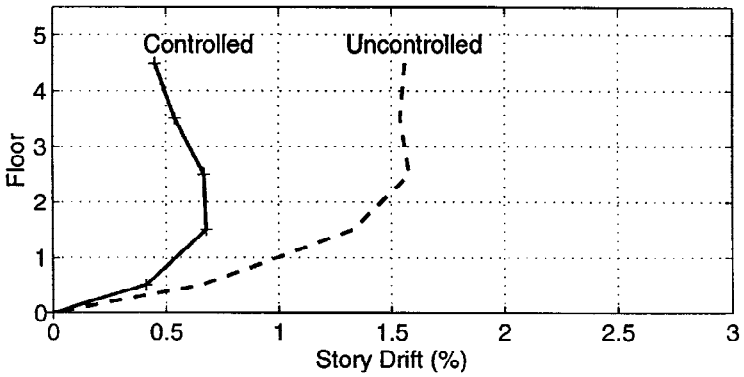

Fig. 5. Peak story drift, showing excellent performance of control.